SUPPLEMENT ARTICLE

Standardizing Scenarios to Assess the Need to Respond to an Influenza Pandemic

Martin I. Meltzer,[1] Manoj Gambhir,[2,3,4] Charisma Y. Atkins,[1] and David L. Swerdlow[3]

[1]Division of Preparedness and Emerging Infections, National Center for Emerging and Zoonotic Infectious Diseases, Centers for Disease Control and Prevention (CDC), Atlanta, Georgia; [2]Epidemiological Modelling Unit, Department of Epidemiology and Preventive Medicine, Monash University, Melbourne, Australia; [3]Modeling Unit and Office of the Director, National Center for Immunization and Respiratory Diseases, CDC, and [4]IHRC, Inc, Atlanta, Georgia

Keywords. standardized scenarios; influenza; pandemic; interventions.

An outbreak of human infections with an avian influenza A(H7N9) virus was first reported in eastern China by the World Health Organization on 1 April 2013 [1]. This novel influenza virus was fatal in approximately one-third of the 135 confirmed cases detected in the 4 months following its initial identification [2], and limited human-to-human H7N9 virus transmission could not be excluded in some Chinese clusters of cases [3, 4]. There was, and still is, the possibility that the virus would mutate to the point where there would be sustained human-to-human transmission. Given that most of the human population has no prior immunity (either due to natural challenge or vaccine induced), such a strain presents the danger of starting an influenza pandemic.

In response to such a threat, the Joint Modeling Unit at the Centers for Disease Control and Prevention (CDC) was asked to conduct a rapid assessment of both the potential burden of unmitigated disease and the possible impacts of different mitigation measures. We were tasked to evaluate the 6 following interventions: invasive mechanical ventilators, influenza antiviral drugs for treatment (but not large-scale prophylaxis), influenza vaccines, respiratory protective devices for healthcare workers and surgical face masks for patients, school closings to reduce transmission, and airport-based screening to identify those ill with novel influenza virus entering the United States. This supplement presents reports on the methods and estimates for the first 5 listed interventions, and in this introduction we outline the general approach and standardized epidemiological assumptions used in all the articles.

METHODS

Approach to Modeling

Given that there had not yet been (and subsequently has not been to date) a pandemic caused by the H7N9 virus, there are no relevant large-population data concerning transmission and clinical impacts of H7N9. We therefore had to consider the potential impacts of disease and interventions for a not fully defined pandemic (ie, a pandemic caused by a generic influenza strain HxNy). Thus, any model that we built had to allow for a wide range in virus transmissibility and resulting clinical impact. The models had to also fully consider a range of effectiveness of interventions—for example, influenza antiviral drugs could be less effective against the next influenza strain causing a pandemic.

Given these uncertainties, and the need for a rapid assessment of a large number of factors, the models produced had to meet a number of specifications: had to be produced in a manner that would allow the models to be easily transferred to other units in government and to public health officials, and subsequently used by people who did not build them; had to provide easy identification of all input variables, their values, and ability to rapidly change those values; can be easily stored and resurrected for future use and reference at some unspecified time in the future; and, the results from each model can

Correspondence: Martin I. Meltzer, PhD, Division of Preparedness and Emerging Infections, National Center for Emerging and Zoonotic Infectious Diseases, Centers for Disease Control and Prevention, Mailstop C-18, 1600 Clifton Rd, Atlanta, GA 30333 (qzm4@cdc.gov).

Clinical Infectious Diseases® 2015;60(S1):S1–8

DOI: 10.1093/cid/civ088

be readily compared to each other. In response to these specifications, we decided to require that each model be built in a spreadsheet format, and that we would essentially have 1 model for each intervention considered.

Meeting these specifications had the added value of producing models that readily fit into the existing CDC Emergency Operations response structure. In this structure, groups called Task Forces are formed to focus on particular aspects of a response to a public health emergency. For example, for an influenza pandemic response, there are usually Task Forces that focus on vaccines (eg, recommendations regarding prioritization of vaccine supplies, issues related to distribution), medical countermeasures (eg, recommendations regarding use of drugs for treatment and prophylaxis, use of personal protective equipment such as face masks), and nonpharmaceutical interventions (eg, recommendations regarding school closures, border security, and screening).

Standardized Epidemiological Scenarios

To allow easy comparison between results (a specification), we standardized a risk space defined by using ranges of transmission and clinical severity from a previously published influenza severity assessment framework (Figure 1) [5]. The framework can be used to plot, and compare to historical data, the relative severity of an influenza pandemic (or nonpandemic influenza season). The framework uses 2 scales: a scale of clinical severity, and a scale of transmissibility. The severity scale has a number of components in it, including case-fatality ratio and case-to-hospitalization ratio (Table 1) [5]. The transmissibility scale is assessed by considering factors such as the clinical (symptomatic) attack rate in various locales, such as school, community, and workplace (Table 1) [5].

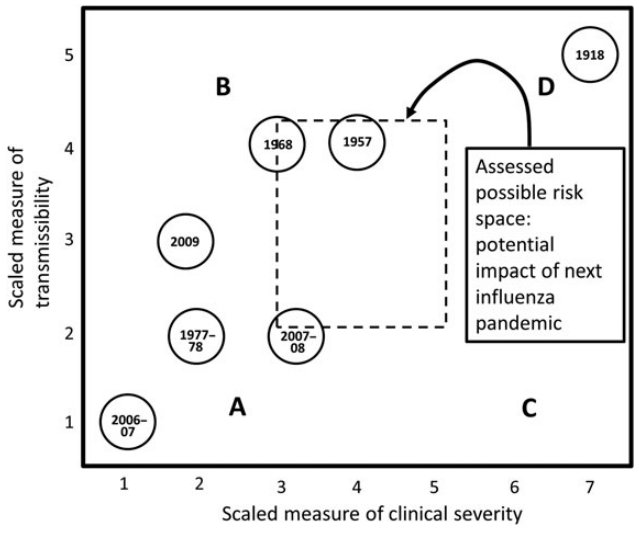

Figure 1. Framework for assessing the impact of an influenza pandemic, with examples of past pandemics and influenza seasons plotted as examples. The assumed possible risk space is the range of possible transmissibility and clinical severity standardized for use in all models used to assess the possible impact of studied interventions. For the actual range of values used in each of the models, see Table 1. See main text for additional details. Note that the 1977–1978, 2006–2007, and 2007–2008 seasons were nonpandemic seasons. They are included to provide reference points regarding the impact of nonpandemic seasons. Adapted from Reed et al [5].

Possible Risk Space

We defined and chose a risk space that has a transmission scale that runs from approximately a scale of 3 (eg, comparable to a community attack rate of 11%–15%) to a scale of 5 (community attack rate of >25%) (Figure 1, Table 1). Our defined risk space has a low-end clinical severity scale of 3, with a case-fatality ratio of 0.05%–0.1% and a death-to-hospitalization ratio of 7%–9% (Table 1). The upper range of severity in our risk space was defined as a scale of 5, with a case-fatality rate of 0.25%–0.5%, and a death-to-hospitalization ratio of 13%–15% (Table 1). Note that the defined risk space encloses the 1968 and 1957 pandemics (Figure 1).

It is essential to note that this chosen risk space is illustrative, not definitive. Until there are data defining the epidemiological elements of the next pandemic, such as rate of transmission, and case-fatality rate, other risk spaces could be chosen for planning purposes. The models presented in this collection, built to the specifications listed here, allow for rapid alterations in input values.

Epidemic Curves

The size and shape of the epidemic curve could impact the effectiveness of interventions. For example, the impact of influenza vaccines depends upon the start of deliveries of large amounts of vaccine compared to the timing of the pandemic peak. Thus, we included in the standardized epidemiological scenario 4 epidemic curves, produced using a simple simulation model (see below). We configured the model using 2 clinical attack rates of approximately 20% and 30%. These clinical attack rates represent the aggregated attack rate across the entire US population. Within the population, subpopulations will typically experience different attack rates (eg, children will experience a higher attack rate than adults 20–64 years old—see description later in paper). Furthermore, for each attack rate, we assumed 2 starting (seeding) scenarios. We used one scenario in which the pandemic started with the arrival of 10 infectious cases and the other when the pandemic started with 100 infectious cases (Figure 2).

To model the 4 epidemic curves, we built a simple, nonprobabilistic (ie, deterministic) model that simulates the spread of influenza through a population by moving the population into groups of susceptible, exposed, infectious, and recovered or death (Table 2 provides values used). We divided the population into 4 age groups (0–10, 11–20, 21–60, or ≥61 years of age). We

Table 1. Measures of Transmissibility and Clinical Severity for the Defined Pandemic Impact Assessment[a]

Parameter		Scale[b] 1	2	3	4	5	6	7
Transmissibility								
1	Symptomatic attack rate, community	≤10%	*11%–15%*	*16%–20%*	*21%–24%*	≥25%		
2	Symptomatic attack rate, school	≤20%	*21%–25%*	*26%–30%*	*31%–35%*	≥36%		
3	Symptomatic attack rate, workplace	≤10%	*11%–15%*	*16%–20%*	*21%–24%*	≥25%		
4	Household secondary attack rate, symptomatic	≤5%	*6%–10%*	*11%–15%*	*16%–20%*	≥21%		
5	R_0: basic reproductive number	≤1.1	*1.2–1.3*	*1.4–1.5*	*1.6–1.7*	≥1.8		
6	Peak % outpatient visits for influenza-like illness	1%–3%	*4%–6%*	*7%–9%*	*10%–12%*	≥13%		
Clinical severity								
1	Case-fatality ratio	<0.02%	0.02%–0.05%	**0.05%–0.1%**	0.1%–0.25%	**0.25%–0.5%**	0.5%–1%	>1%
2	Case-hospitalization ratio	<0.5%	0.5%–0.8%	**0.8%–1.5%**	1.5%–3%	**3%–5%**	5%–7%	>7%
3	Ratio, deaths: hospitalization	≤3%	4%–6%	**7%–9%**	10%–12%	**13%–15%**	16%–18%	>18%

For case-fatality ratio and case-hospitalized ratio, scale 3 shows low severity, and scale 5 shows high severity (in bold).

Source: Adapted from Reed et al [5].

[a] These estimates related to the framework for assessing the impact of influenza pandemics, shown in Figure 1.

[b] Italics represent the measures of transmissibility included in the defined risk space, shown in Figure 1.

modeled the probabilities of daily contact (and thus risk of disease transmission) by constructing a contact matrix using data from the United Kingdom (see Table A1 in Technical Appendix A).

We thus produced 4 notably different epidemic curves (Figure 2). For example, the two 30% attack rate scenarios peak in weeks 12 and 14, whereas the 20% attack rate scenarios peak in weeks 13 and 22 (Figure 2). The clinical attack rates by age group are presented in Table 3. Obviously, the largest numbers of cases occur in the largest age group of 21- to 60-year-olds; however, children in both the 0–10 and 11–20 age groups have the highest attack rates, indicating a potentially greater degree of vulnerability (Table 3).

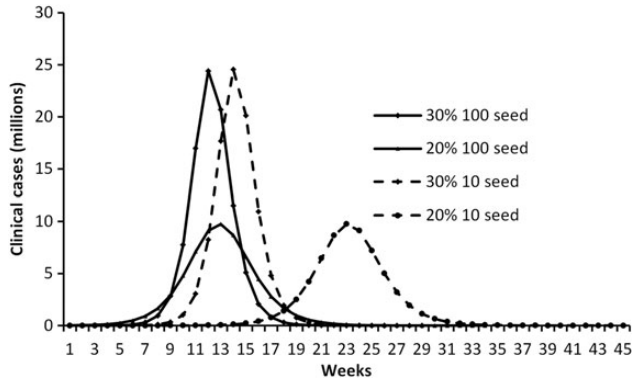

Figure 2. Standardized attack rates and epidemic curves used in the models: 2 clinical attack rates and 2 initial seedings. Clinical attack rates of 20% or 30% represent the aggregated attack rate across the entire US population. A 30% clinical attack rate results in approximately 94 million persons becoming ill, and a 20% clinical attack rate causes approximately 64 million to become ill. Within the population, subpopulations will typically experience different attack rates (see Table 3). Seeding refers to the number of infectious cases, either 10 or 100, that arrives near-simultaneously in the United States to start the pandemic.

Strengths and Limitations

Perhaps one of the greatest strengths of the simple models presented in this collection of articles is that they highlight what is

Table 2. Assumed Values Used to Model the Standardized Influenza Epidemiological Curves

Model Parameter	Value
No. of persons infected per infectious person: for clinical attack rate of 20%[a]	1.3
No. of persons infected per infectious person: for clinical attack rate of 30%[a]	1.65
Average duration of incubation of infection	1.5 d
Average duration of infectious period	2 d
Proportion of population asymptomatic	50%
Contact mixing matrix	See Technical Appendix A
Initial population immunity	Zero for all age groups

[a] Average number of persons infected per infectious person is often, in modeling terms, referred to as R_0. This number represents the number infected when all, or almost all, of the population is susceptible to infection.

Table 3. Age-Specific Number of Clinical Cases and Attack Rates by Total Population Attack Rate Scenarios

	0–10 y		11–20 y		21–60 y		≥61 y		
Total Clinical Attack Rate	Million Cases	Age-Specific Attack Rate	Million Cases	Age-Specific Attack Rate	Million Cases	Age-Specific Attack Rate	Million Cases	Age-Specific Attack Rate	Total Million Cases
30%	13.1	31.9%	16.9	39.0%	52.7	31.0%	11.3	20.0%	94.0
20%	8.9	21.7%	12.7	29.3%	35.2	20.7%	6.9	12.2%	63.7

and is not known about the burden of disease and the potential impact of a planned intervention. To find the weaknesses of what is currently known, a reader need only consult Table 1 in each article. These tables list inputs, their assumed values, and data sources. An example of an important unknown is as follows: When estimating the number of respiratory protection devices (eg, face and surgical masks) needed by first responders (police officers, firefighters, emergency medical technicians), one could assume that first responders will need 1 mask per person whom they encounter with influenza-like illness. The problem is that there are no readily available data that report on the measurement of such [6]. Similarly, when considering the potential use and impact of influenza antiviral drugs, O'Hagan et al had to assume that existing influenza antiviral drugs would have the same level of effectiveness against the strain causing the next influenza pandemic as they do with existing influenza strains [7]. Despite these limitations, these simple models make it fairly straightforward to rapidly assess the relative importance of each of the input variables.

One assumption that may not be readily appreciated is the impact of the shape of the standardized epidemiological curves used in all the models (Figure 2). Previous influenza pandemics have produced different shapes of deaths over time (Figure 3). Such differences in deaths over time can greatly influence the success of some of the interventions. For example, when considering the number of mechanical ventilators needed at the peak of the pandemic, Meltzer et al initially assumed that the peak demand for ventilators would equal approximately 13% of all patients needing mechanical ventilation [8]. However, in the 30% attack rate epidemiological curve (Figure 2), the number of cases that

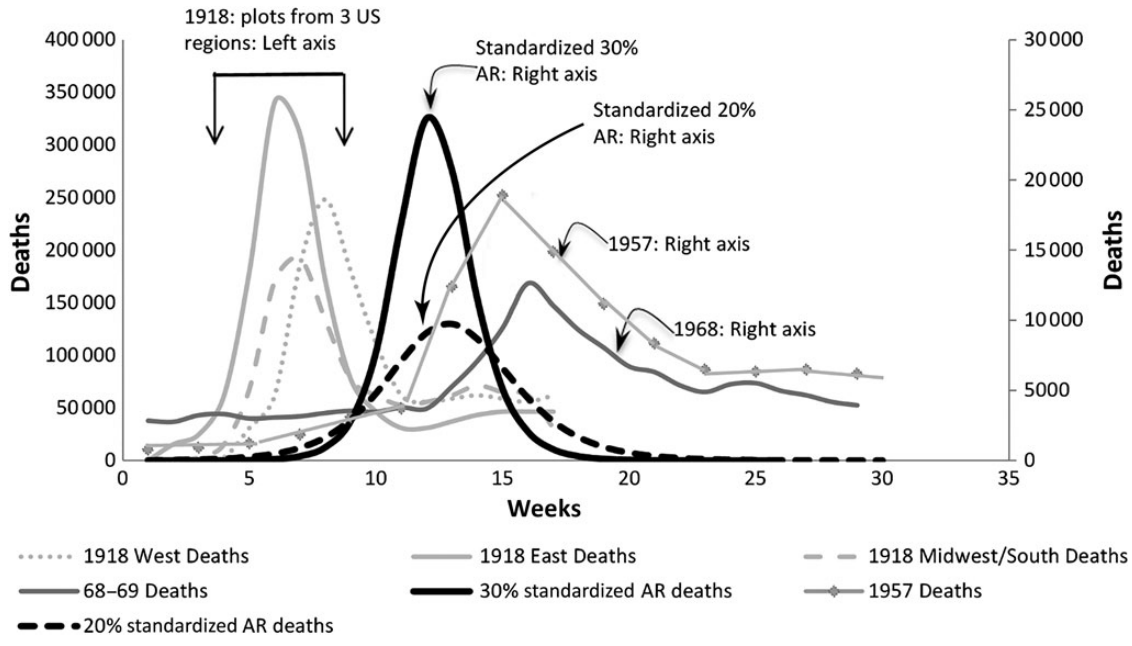

Figure 3. Standardized plots of deaths over time from different influenza pandemics compared to the epidemic curves used in the model. The different curves illustrate that influenza pandemics can have different pattern of deaths (and, by extension, cases) over time. When the peak occurs and the shape of the curve can greatly influence the success of some of the interventions. See main text and Technical Appendix B for further details. These curves were standardized to the approximate 2014 US population of 310 million persons. The standardized curves of 20% and 30% attack rate (AR) refer to the curves built for this exercise. The 2 standardized curves plotted here are those assuming an introduction of 100 infectious persons (*cf*, Figure 2). Note that the data for 1957 were recorded once every 2 weeks, whereas all other plots used weekly data. See Technical Appendix B for further details.

occur in the peak 10 days is approximately 30% of all cases. Thus, the authors of the ventilator study conducted a sensitivity analysis by changing from 13% to 30% the assumed number of mechanically ventilated patients that occurs at the peak of a pandemic.

The articles in this supplement also incorporate other important implicit assumptions. One of the more important is that each article essentially assumes that the healthcare system can absorb and/ or successfully execute any of the interventions so modeled. For example, Biggerstaff et al provide some estimates of the impact of influenza vaccination in which it was assumed that 30 million persons could be vaccinated each week [9]. The US private and public health systems, collectively or separately, have never previously achieved such a rate (though the authors clearly demonstrate that achieving such a rate would have very positive public health outcomes).

Furthermore, the successful deployment and ultimate impact of each intervention is likely to have a wide variation. Schools can close for different lengths of time, antiviral drug prescription and distribution may not be equally efficient in all areas, and healthcare workers and patients may have different levels of compliance in wearing protective gear.

Finally, readers will note that there are no reports in this collection that consider the simultaneous deployment of ≥2 interventions. It is realistic to assume that, during the next influenza pandemic, public health officials, healthcare providers, and other policy makers are likely to enact several interventions at once (eg, close schools, start dispensing antiviral medications, recommend use of protective personal gear). The problem arises in that such multi-intervention models become very scenario specific. For example, different locales are likely to face different unmitigated epidemic curves (Figure 3). Thus, researchers who estimate the potential impact of combining several interventions at once have to make a very large increase in the number of assumptions. This makes it more difficult to both generalize the results and to rapidly understand what assumptions are relatively more important.

Despite these limitations, we believe that the benefits of using these models outweigh the limitations. This assessment is based on our experience of using the models and results produced to help public health leadership reassess US influenza pandemic planning and preparedness. In the 2013 response to the H7N9 threat, the most important outcome from policy makers seeing the results from these models was the intense debate concerning the inputs and assumptions. We thus believe that the methodology used here to develop and guide the building of the models in this collection, and the subsequent interpretations and use of the results, can be a useful part of future public health responses.

Supplementary Data

Supplementary materials are available at *Clinical Infectious Diseases* online (http://cid.oxfordjournals.org). Supplementary materials consist of data provided by the author that are published to benefit the reader. The posted materials are not copyedited. The contents of all supplementary data are the sole responsibility of the authors. Questions or messages regarding errors should be addressed to the author.

Notes

Disclaimer. The findings and conclusions in this report are those of the authors and do not necessarily represent the official position of the Centers for Disease Control and Prevention (CDC).

Financial support. M. I. M., C. Y. A., and D. L. S. conducted this research as part of their usual duties as employees of the CDC. M. G. was funded through a grant from the US National Institutes of Health, National Institute of General Medical Sciences (grant number 1U01GM110721-01).

Supplement sponsorship. This article appears as part of the supplement titled "CDC Modeling Efforts in Response to a Potential Public Health Emergency: Influenza A(H7N9) as an Example," sponsored by the CDC.

Potential conflicts of interest. All authors: No reported conflicts.

All authors have submitted the ICMJE Form for Disclosure of Potential Conflicts of Interest. Conflicts that the editors consider relevant to the content of the manuscript have been disclosed.

References

1. World Health Organization. Human infection with influenza A(H7N9) virus in China, **2013**. Available at: http://www.who.int/csr/don/2013_04_01/en/index.html. Accessed 5 September 2013.
2. World Health Organization. Human infection with avian influenza A (H7N9) virus—update, **2013**. Available at: http://www.who.int/csr/don/2013_08_11/en/index.html. Accessed 5 September 2013.
3. Li Q, Zhou L, Zhou M, et al. Epidemiology of human infections with avian influenza A(H7N9) virus in China. N Engl J Med **2014**; 370: 520–32.
4. Qi X, Qian YH, Bao CJ, et al. Probable person to person transmission of novel avian influenza A (H7N9) virus in eastern China, 2013: epidemiological investigation. BMJ **2013**; 347:f4752.
5. Reed C, Biggerstaff M, Finelli L, et al. Novel framework for assessing epidemiologic effects of influenza epidemics and pandemics. Emerg Infect Dis **2013**; 19:85–91.
6. Carias C, Rainisch G, Shankar M, et al. Potential demand for respirators and surgical masks during a hypothetical influenza pandemic in the United States. Clin Infect Dis **2015**; 60(suppl 1):S42–51.
7. O'Hagan JJ, Wong KK, Campbell AP, et al. Estimating the United States demand for influenza antivirals and the effect on severe influenza disease during a potential pandemic. Clin Infect Dis **2015**; 60(suppl 1): S30–41.
8. Meltzer MI, Patel A, Ajao A, Nystrom SV, Koonin LM. Estimates of the demand for mechanical ventilation in the United States during an influenza pandemic. Clin Infect Dis **2015**; 60(suppl 1):S52–7.
9. Biggerstaff M, Reed C, Swerdlow DL, et al. Estimating the potential effects of a vaccine program against an emerging influenza pandemic—United States. Clin Infect Dis **2015**; 60(suppl 1):S20–9.
10. Mossong J, Hens N, Jit M, et al. Social contacts and mixing patterns relevant to the spread of infectious diseases. PLoS Med **2008**; 5: e74.
11. Markel H, Lipman HB, Navarro JA, et al. Nonpharmaceutical interventions implemented by US cities during the 1918–1919 influenza pandemic. JAMA **2007**; 298:644–54.
12. Epidemiology Branch. The epidemiology of Asian influenza. 1957–1960. A descriptive brochure. Atlanta, Georgia: Communicable Disease Center, **1960**.
13. Sharrar RG. National influenza experience in the U.S., 1968–1969. Bull World Health Org **1969**; 41:361–6.
14. Meltzer MI, Cox NJ, Fukuda K. The economic impact of pandemic influenza in the United States: priorities for intervention. Emerg Infect Dis **1999**; 5:659–71.

APPENDIX

TECHNICAL APPENDIX A: CONTACT MATRIX FOR EPIDEMIOLOGICAL MODEL

Standardized epidemiological curves—contact matrix: To model the 4 epidemic curves (Figure 2), we built a simple, nonprobabilistic (ie, deterministic) model in which we divided the population into 4 age groups (0–10, 11–20, 21–60, ≥61 years). To measure the risk of contact and possible onward spread between and within each age group, we used the contact matrix shown in Table A1. For the contact matrix, we used, in the absence of relevant data from the United States, data from the United Kingdom [10], collected as part of a study called the Polymod study that collected contact data from approximately 8000 persons living in 8 European countries [10]. Because the UK data are split into 5-year age groups, we had to aggregate the data into the 4 age groups used in our model. During this aggregation, we ensured that the total number of contacts between any 2 age groups is "equal in any direction" (eg, the number of contacts between 0–9 years and 10–18 years is the same as those between 10–18 years and 0–9 years). We used, for this aggregation process, the age distribution of the US population (www.censusscope.org).

Recalibrating the Mixing Matrix Into 4 Age Groups

As noted above, the UK contact data [10] are split into 5-year age groups, which we had to aggregate into the 4 age groups used in our models. Furthermore, the matrix that we constructed had to meet the condition of being symmetrical. That is, the number of contacts from age group A to age group B should equal the number of contacts in the reverse direction.

We begin the explanation of how we built our contact matrix by introducing some notation: The mixing matrix elements of the published matrix [10] are denoted by θ_{ij}, $i, j = 1, \ldots, m$, where i, j refers to rows and columns, respectively, and m is the number of age groups in the mixing matrix.

As the mixing matrix required has fewer age groups than that of the published Polymod matrix [10], indexed by $f, g = 1, \ldots, n$, then we let age group u contain narrower age groups $i = l(f)$ to $u(f)$.

1. The contact rate between someone in group i and another in group g is given by

$$d_{ig} = \sum_{j=l(g)}^{u(g)} \theta_{ij}.$$

We then proceed according to the following steps:

2. If the US population distribution is such that the population in age group i is N_i, we can calculate the population-weighted means of each of the elements d, to obtain contact rates between groups f and g. For $f = g$, this calculation is simple:

$$e_{ff} = \frac{\sum_{i=l(f)}^{u(f)} N_i d_{if}}{\sum_{i=l(f)}^{u(f)} N_i}.$$

3. For the elements that are off the diagonal, the calculation becomes more complicated because we need to sum up the correct number of contacts made between each age group. The total reported rates of contact from f to g and g to f are:

$$Y_{fg} = \sum_{i=l(f)}^{u(f)} N_i d_{ig}$$

$$Y_{gf} = \sum_{i=l(g)}^{u(g)} N_i d_{if}.$$

4. Theoretically, these values should be equal to one another; however, they differ from one another when calculated from actual reported contact rates (from self-administered surveys such as those conducted by Mossong et al [10]), and so, to ensure that they are equal, we can average them before calculating the final mixing-matrix elements e_{fg} and e_{gf}:

$$Z_{fg} = \frac{(Y_{fg} + Y_{gf})}{2}$$

$$e_{fg} = \frac{Z_{fg}}{\sum_{i=l(f)}^{u(f)} N_i}, \quad e_{gf} = \frac{Z_{fg}}{\sum_{i=l(g)}^{u(g)} N_i}.$$

Here then, e_{fg} is the rate at which an individual in age group f makes contacts with anyone in age group g, per unit time, as reported in the original data (ie, per day for the original Mossong et al [10] data).

An example of this procedure is given below, following the steps above, outlined theoretically:

1. We begin with the "all contacts" (ie, both conversational and physical) matrix for Great Britain from the Polymod

Table A1. Contact Matrix Used to Model Probabilities of Contact and Potential Onward Transmission Between Age Groups (Contacts per Day Between Each Age Group)

	No. of Contacts per Day			
	Age Groups, y			
Age group, y	0–10	11–20	21–60	≥61
0–10	4.962	1.235	5.029	0.743
11–20	1.197	8.063	5.640	1.018
21–60	1.102	1.275	7.582	1.488
≥61	0.389	0.55	3.556	2.254

Source: Adapted from Mossong et al [10] (Supplementary Table 8.4: contact data from Great Britain).

study. The elements of this matrix denote the daily number of contacts between an individual in one 5-year age group with those in another 5-year age group. Element (1,2), for example, is the daily number of contacts a person aged 0–4 years has with someone aged 5–9 years. The fill matrix is as follows:

1.9	0.7	0.4	0.2	0.5	0.7	0.7	0.8	0.2	0.2	0.4	0.2	0.2	0.3	0.1
1.0	6.6	1.1	0.7	0.6	0.8	1.0	1.4	0.9	0.2	0.3	0.2	0.5	0.5	0.2
0.5	1.3	6.9	1.5	0.3	0.3	0.5	0.8	1.0	0.7	0.3	0.4	0.3	0.4	0.3
0.3	0.3	1.0	6.7	1.6	0.7	0.4	0.6	0.9	1.2	0.7	0.3	0.2	0.5	0.6
0.5	0.3	0.2	0.9	2.6	1.5	0.8	0.6	0.8	0.9	0.9	0.6	0.5	0.4	0.3
0.8	0.7	0.4	0.7	1.3	1.8	1.0	0.7	0.7	0.9	0.9	0.9	0.7	0.7	0.3
1.0	1.1	0.6	0.5	0.9	1.2	1.7	0.9	1.0	0.9	0.9	0.6	0.8	0.6	0.3
1.0	1.0	1.3	1.1	0.8	1.0	1.5	1.5	1.3	1.1	0.8	0.7	1.0	1.0	0.2
0.6	1.0	1.1	0.9	0.7	0.9	0.8	1.2	1.4	1.3	0.9	0.7	0.9	0.8	0.8
0.3	0.5	0.6	0.8	1.0	0.9	0.6	0.8	1.3	1.9	0.6	0.8	0.6	0.6	0.6
0.3	0.4	0.4	0.4	0.4	0.9	0.6	0.6	0.7	1.0	0.7	1.1	0.6	0.6	0.6
0.3	0.2	0.3	0.3	0.4	0.5	0.7	0.5	0.6	0.5	0.8	1.2	0.9	0.9	0.3
0.3	0.3	0.2	0.2	0.2	0.3	0.4	0.4	0.5	0.6	0.4	0.8	0.7	0.9	0.6
0.1	0.1	0.1	0.2	0.2	0.2	0.1	0.3	0.2	0.1	0.2	0.3	0.4	0.7	0.6
0.1	0.2	0.2	0.1	0.2	0.2	0.2	0.4	0.5	0.7	0.5	0.8	0.5	0.7	1.5

Summing the columns of the 5-year group matrix according to the desired group widths (eg, the first 2 columns are summed to give a 10-year age group column) gives the following intermediate 15-group by 4-group matrix:

2.6	0.7	3.7	0.6
7.6	1.8	5.3	1.2
1.8	8.4	4.3	1.0
0.7	7.7	6.3	1.3
0.8	1.2	8.6	1.2
1.5	1.2	8.1	1.7
2.0	1.1	8.1	1.7
2.0	2.4	8.7	2.2
1.6	2.1	7.8	2.6
0.8	1.3	7.9	1.8
0.7	0.8	6.0	1.7
0.5	0.6	5.2	2.0
0.5	0.4	3.5	2.1
0.2	0.3	1.7	1.7
0.3	0.3	3.5	2.7

2. Next, we obtain a vector whose elements are the numbers of individuals in each of the age groups of the original matrix (here 5-year width groups, taken from the 2011 Great Britain census; the age distribution should correspond closely with the distribution that held at the time when the contact survey was performed), and we perform a sum of the total number of contacts to produce an aggregated age group (ie, two 5-year age groups are aggregated into one 10-year age group).

3 914 000 (eg, first row is the number of individuals in the age group 0–4 years).
3 517 000
3 669 000
3 997 000
4 297 000
4 307 000
4 126 000
4 194 000
4 624 000
4 643 000
4 095 000
3 614 000
3 808 000
3 019 000
2 463 000
2 006 000
1 498 000
918 000
476 000

For example, to construct the matrix element pertaining to the total number of contacts between the 0–9-year age group and the 0–9-year age group (ie, itself), we perform the following sum:

$$3\,914\,000 * 2.6 + 3\,517\,000 * 7.6 = 36\,905\,600.$$

This is the first diagonal element of the "total contacts" matrix and, again, it represents the total number of contacts made per day between those in the 0–9-year age group.

Because diagonal elements are of course the same as their off-diagonal counterparts, there is no problem.

3. However, corresponding pairs of off-diagonal totals should be the same; that is, the total number of contacts between those in the 0–9-year and 10–19-year groups should be the same as the total number between those in the 10–19-year and 0–9-year age groups.

Y21 = N3*d31 + N4*d41 = 3 669 000*1.8 + 3 997 000*0.7 = 9 402 100
Y12 = N1*d12 + N2*d22 = 3 914 000*0.7 + 3 517 000*1.8 = 9 070 400

36 753 010	8 945 040	33 090 700	6 459 320
9 245 500	61 646 310	40 847 730	8 941 760
42 080 560	45 753 440	257 630 820	63 160 700
3 260 150	3 367 050	27 090 960	19 494 940

These 2 total contact numbers are not the same and so we take the average of them and they become the (1,2) and (2,1)

elements of the total contact matrix. Note that the numbers in the above matrix in these 2 positions differ slightly from those in the Y21, Y22 calculations outlined above; this is because daily Polymod contacts were rounded for the calculations illustrated.

4. Once we have completed this procedure for the whole aggregated total contact matrix, we need to divide our total contact numbers by the correct number of individuals in each age group, to ensure we end up with a matrix that gives the number of contacts per person per day in the relevant age group.

For example, the (1,1) element of the final matrix is the (1,1) element of the matrix produced by step (2) divided by the total number of individuals in the first age group (ie, the sum of the individuals in the first two 5-year age groups = 3 914 000 + 3 517 000 = 7 431 000); and the (1,2) element is divided by the same number, whereas the (2,1) element is divided by the number in the second age group = 3 669 000 + 3 997 000 = 7 666 000. Dividing through gives the final matrix below (which is similar to Table A1, accounting for rounding in the illustrative calculation).

4.9	1.2	5.1	0.7
1.2	8.0	5.6	0.8
1.1	1.3	7.6	1.3
0.4	0.7	4.9	2.1

TECHNICAL APPENDIX B: DATA AND NOTES FOR FIGURE 3

To model the curves shown in Figure 3, we used the estimated number of deaths from previous pandemic seasons (1918, 1957, and 1968). We compared those to the estimated clinical cases from the epidemiological model built for this exercise, using attack rates of both 20% and 30% (ie, the curves shown in Figure 2, main text). All deaths were based on the clinical data reported during the specific pandemic season. However, in an effort to obtain current death estimates, we extrapolated the seasonal case values (either clinical data or number of deaths) into current-year 2014 US cases at a total population of 310 million.

- 1918 influenza pandemic: We obtained from the source [11] the weekly number of deaths in 1918 (per 100 000 people) for the reported 3 different US geographic locations (West, East, and Midwest/South). We then adjusted those number of deaths, per 100 000, to the approximate current US population of 310 million persons (ie, multiplied each data point by 3100). This gave us the equivalent number of deaths for the 2014 US population.
- 1957 influenza pandemic: We obtained the total, all ages biweekly (ie, reported every 2 weeks) number of respiratory illnesses per 100 000 from Figure 5 in the report of the CDC (then known as the Communicable Disease Center) [12]. We then adjusted those number of cases to the approximate current US population of 310 million persons (ie, multiplied each data point by 3100). This gave us the equivalent number of cases for the 2014 US population. To obtain estimates of deaths in equivalent 2014 US population, we multiplied the estimates of cases by a case-fatality ratio of 0.001 (ie, 0.1% of all cases result in death). This case-fatality estimate was taken from Table 1 in the main text [5].
- 1968 influenza pandemic: We obtained the weekly reported number of pneumonia-influenza deaths in 122 US cities from Figure 3 in Sharrar et al [13]. However, the total number of deaths recorded by Sharrar et al was only 19 450, which is notably lower than what may be expected. We therefore used a multiplier of 7.89 to adjust upward their estimates. We constructed this multiplier by noting that Meltzer et al's Figure 1 [14] showed approximately 155 000 deaths for a 1968-type influenza pandemic occurring in the US population (ie, 155 000/19 540 = 7.89).
- Attack rates: We took the 2 curves plotting the 20% and 30% clinical case attack rates shown in Figure–2 of the main text (the 2 plots assuming 100 infectious persons start, or "seed," the pandemic in the United States). We then used a case-fatality rate of 0.001 (ie, 0.1% of all cases result in death), taken from Table 1 in the main text [5]. For simplicity, we assumed a low severity (scale of 3) of 0.1% for both attack rates to generate the number of deaths.